Available online at www.sciencedirect.com
SCIENCE DIRECT®
Bioorganic & Medicinal Chemistry 14 (2006) 2082–2088
Bioorganic & Medicinal Chemistry

Effective discrimination of antimalarial potency of artemisinin compounds based on quantum chemical calculations of their reaction mechanism

Somsak Tonmunphean, Vudhichai Parasuk and Sirirat Kokpol*

Department of Chemistry, Faculty of Science, Chulalongkorn University, Patumwan, Bangkok 10330, Thailand

Received 16 June 2005; revised 8 July 2005; accepted 8 July 2005
Available online 7 February 2006

Abstract—The reaction mechanism of 12 antimalarial artemisinin compounds with two competitive pathways was studied by means of quantum chemical calculations using the IMOMO(B3LYP/6-31(d,p):HF/3-21G) method. The oxygen-centered radicals, carbon-centered radicals, and transition states (TS) in both pathways were geometrically optimized. The obtained kinetic and thermodynamic energy profiles show that homolytic C–C cleavage reaction (pathway 2) is energetically more preferable than an intramolecular 1,5-hydrogen shift process (pathway 1), which is consistent with the docking calculations. However, compounds that can easily proceed along the pathway 1 have high activity. Therefore, both pathways are important for antimalarial activity. Moreover, effective discrimination between high and low activity compounds using EA_1, ΔE_1, and $\Delta E(1A - 2A)$ was accomplished.
© 2005 Elsevier Ltd. All rights reserved.

1. Introduction

Malaria continues to be a critical problem worldwide owing to the emergence of resistance strains of malarial parasites to almost all available antimalarial drugs.[1] Therefore, there is great need for new effective chemotherapeutic agents. The development of a new drug is a very long and expensive process. It is thus ideal to have a method that enables a prediction of biological activity of new compounds in advance based on the knowledge of chemical structure alone, for example, quantitative structure–activity relationship (QSAR) technique,[2,3] because this would bring down the number of analogues that have to be made and it greatly reduces the syntheses and testing biological activity efforts. Definitely, this will save a lot of time and money. In this paper, such a prediction method was developed for antimalarial artemisinin compounds.

Artemisinin (Fig. 1A) and its derivatives are the only group of compounds that are still effective against drug-resistant strains of malaria and thus the development of new antimalarial drugs is essentially based on these compounds. The most interesting point is why artemisinin compounds are still effective, while the others are not. One possible reason could be that they have a mode of action different from other antimalarial drugs as a consequence of their unusual structures. Therefore, our attentions were focused on their reaction mechanisms.

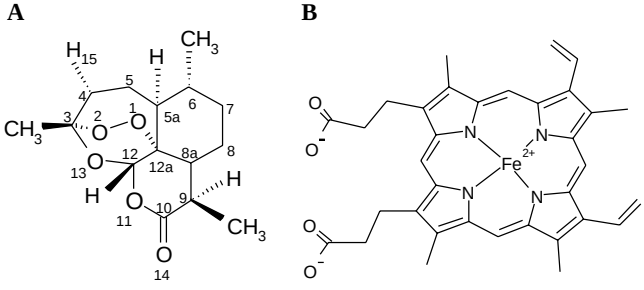

Figure 1. Structure of (A) artemisinin with atom numbering and (B) heme molecule.

Although the mechanism of action of artemisinins is still not conclusive, there are strong evidences[4–6] to suggest that an endoperoxide linkage of artemisinins and a heme

Keywords: Mechanism of action; Antimalarial activity; Endoperoxide; Transition state.
* Corresponding author. Tel.: +662 218 7583; fax: +662 218 7598; e-mail: sirirat.k@chula.ac.th

0968-0896/$ - see front matter © 2005 Elsevier Ltd. All rights reserved.
doi:10.1016/j.bmc.2005.07.003

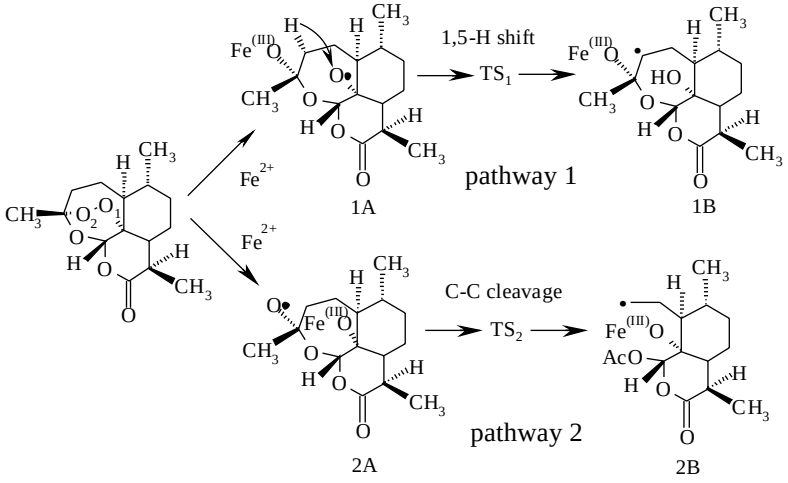

Figure 2. Proposed mechanism of action of artemisinin compound.

iron play critical roles in their reaction mechanism, which was suggested to comprise of two distinct steps.[7–9] In the first step, the activation step, the heme iron (Fig. 1B) attacks and breaks the endoperoxide linkage of artemisinin to produce an oxy free radical, which is then rearranged to give a carbon free radical. In the second step, the alkylation step, the carbon free radical produced from the first step will alkylate specific malarial proteins causing lethal damage to malarial parasites.[10]

For the activation step, there are two possible pathways, pathway 1 and pathway 2 (Fig. 2). In pathway 1, the heme iron attacks the endoperoxide moiety at the O_2 position, giving the free radical at the O_1 position (1A). This process is followed by an intramolecular 1,5-H shift and the C_4 free radical (1B) is obtained. In pathway 2, the heme iron, on the other hand, attacks the endoperoxide moiety at the O_1 position, giving the free radical at the O_2 position (2A). This process is followed by a homolytic cleavage of the C_3–C_4 bond, also resulting in the C_4 free radical (2B). Hence, it could be concluded that the C_4 free radical product is very critical for antimalarial activity of artemisinins.

Table 1. Antimalarial activities of 12 artemisinin compounds

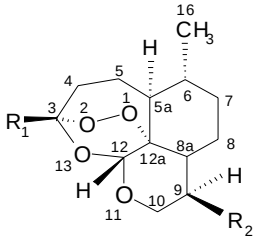

No	R_1	R_2	log (D-6)	log (W-2)
1	CH_3	CH_3	0.819	0.754
2	CH_3	H	0.375	0.279
3	CH_3	CH_2CH_3	0.961	0.668
4	CH_3	$(CH_2)_2CH_3$	0.675	0.740
5	CH_3	$(CH_2)_3CH_3$	1.765	1.320
6	CH_3	$(CH_2)_4CH_3$	0.230	0.161
7	CH_3	$(CH_2)_3C_6H_5$	1.705	1.399
8	CH_2CH_3	H	−1.000	−1.000
9	$(CH_2)_2CH_3$	H	0.859	0.836
10	$CH_2CH(CH_3)_2$	H	0.262	0.398
11	$(CH_2)_2C_6H_5$	H	−1.222	−1.699
12	$(CH_2)_2COOH$	H	−3.046	−3.046

Our previous theoretical study on reaction mechanisms of artemisinin, dihydroartemisinin, and 10-deoxoartemisinin has revealed that these three structurally different compounds exhibit dissimilar energy profiles, which are possibly related to their antimalarial activities.[11] Therefore, further investigations of the thermodynamics and kinetics of the reactions, leading to the formation of C_4 free radical on a greater number of compounds, were carried out to determine their relationship with activity, which can fulfill our goal for the prediction of biological activity of new compounds in advance. From experimental data,[12] it can be seen that substituent group at the C_{10} position seems to have no significant effect on antimalarial activities since most compounds without the substituent have even higher activities than compounds with the substituent. Consequently, 12 compounds without the substituent (10-deoxoartemisinin derivatives)[12] were considered. Their structures and antimalarial activities are shown in Table 1. For comparison purpose, a 6,7,8-trioxybicylco[3,2,2]nonane compound, which was used as the representative model of artemisinin in the previous studies,[13,14] was additionally included in this work.

2. Results and discussion

2.1. Intramolecular 1,5-hydrogen shift (pathway 1)

The optimized structures of O-centered radicals (1A), C-centered (1B) radicals, and transition state (TS_1) for all 12 compounds are shown in Figure 3. Some important structural parameters in radical 1A, transition state TS_1, and radical 1B of 12 artemisinin compounds, as well as a model system, are given in Table 2. Since some structural data of the model system were not reported in

Figure 3. Optimized structures of the (A) O-centered radical 1A, (B) transition state TS_1, and (C) C-centered radical 1B in pathway 1 for all 12 compounds.

Table 2. Important structural parameters of radical 1A, transition state (TS_1), and radical 1B in pathway 1; distances in Angstroms and angles in degrees

		1	2	3	4	5	6	7	8	9	10	11	12	Model
O_1–H_{15}	1A	2.381	2.320	2.318	2.340	2.307	2.303	2.340	2.168	2.452	2.508	2.172	2.171	2.479
	TS_1	1.299	1.285	1.288	1.288	1.288	1.288	1.288	1.290	1.288	1.293	1.288	1.281	1.245
	1B	0.976	0.976	0.976	0.976	0.976	0.976	0.976	0.976	0.976	0.976	0.976	0.975	0.972
O_1–C_4	1A	2.842	2.842	2.836	2.844	2.832	2.831	2.845	2.719	2.870	2.908	2.720	2.718	3.123
	TS_1	2.422	2.409	2.410	2.411	2.410	2.410	2.410	2.412	2.411	2.414	2.411	2.409	2.424
	1B	2.792	2.793	2.789	2.785	2.787	2.787	2.789	2.800	2.798	2.831	2.795	2.797	3.001
C_4–H_{15}	1A	1.092	1.093	1.093	1.093	1.093	1.093	1.093	1.098	1.092	1.093	1.098	1.097	1.097
	TS_1	1.239	1.250	1.247	1.248	1.248	1.248	1.248	1.247	1.248	1.246	1.249	1.253	1.285
	1B	2.484	2.532	2.522	2.524	2.523	2.523	2.518	2.498	2.507	2.502	2.490	2.477	2.593
O_2–H_{15}	1A	2.353	2.362	2.363	2.361	2.365	2.365	2.362	2.490	2.363	2.360	2.492	2.494	2.491
	TS_1	2.411	2.425	2.426	2.487	2.487	2.487	2.489	2.477	2.479	2.457	2.480	2.482	2.571
	1B	1.810	1.826	1.822	1.823	1.825	1.826	1.818	1.817	1.823	1.792	1.825	1.828	1.904
O_1–H_{15}–C_4	1A	103.5	107.2	106.9	106.1	107.4	107.5	106.1	108.2	101.1	100.2	108.0	108.0	116.3
	TS_1	145.1	143.7	143.8	143.8	143.8	143.8	143.8	143.9	143.9	143.9	143.7	143.9	146.7
	1B	98.0	95.1	95.4	95.0	95.3	95.2	95.7	97.7	96.9	99.5	97.8	98.8	105.4

the references,[13,14] this compound was recalculated and its structural data were used in this work.

For the radical 1A, the distance between H_{15} (transferred hydrogen atom) and the radical site O_1 ranges from 2.168 to 2.508 Å, compared to 2.479 Å in the model system. The O_1–H_{15}–C_4 angle in artemisinin compounds (100.2–108.2°) is significantly different from that in the model system (116.3°), that is, around 8–16° less. Moreover, the O_1–C_4 distance in the model system (3.123 Å) is too long compared to those of artemisinin compounds (2.718 to 2.908 Å). The differences in the O_1–H_{15}–C_4 angle and in the O_1–C_4 distance between artemisinin compounds and the model system have clearly arisen from an additional ring strain of the real system. Interestingly, differences in the O_1–H_{15} distance and in the O_1–C_4 distance between high activity compounds (compounds **1**–**7**, **9**, and **10**) and low activity compounds (compounds **8**, **11**, and **12**) were observed. The values of these two distances in low activity compounds are around 0.1–0.3 Å, shorter than those in high activity compounds. In the transition state TS_1, the H_{15} atom was moved toward the O_1 atom, reducing the O_1–H_{15} distance to be in the range of 1.281–1.299 Å. The O_1–H_{15}–C_4 angle in artemisinin compounds is around 144–145°, which again ensures that the collinear transition state is not necessary.[14,15] For the radical 1B, the H_{15} atom is placed close to the O_2 atom, giving a distance of 1.792–1.828 Å, in which the hydrogen bonding can take place.

The activation energy (EA_1) and the energy difference between radical 1A and 1B (ΔE_1) for all 12 compounds and the model system are given in Table 3. Interestingly, significant differences in energy values between high and low activity compounds were discovered. The energy

Table 3. Activation energy (EA_1) and energy difference between radical 1A and 1B (ΔE_1) in pathway 1

No	log (D-6)	log (W-2)	EA_1 (kcal/mol)	ΔE_1 (kcal/mol)
1	0.819	0.754	4.67	−9.75
2	0.375	0.279	4.71	−9.68
3	0.961	0.668	4.65	−9.72
4	0.675	0.740	4.66	−9.73
5	1.765	1.320	4.66	−9.71
6	0.230	0.161	4.66	−9.71
7	1.705	1.399	4.64	−9.80
8	−1.000	−1.000	7.29	−6.70
9	0.859	0.836	4.78	−9.12
10	0.262	0.398	4.59	−9.38
11	−1.222	−1.699	7.35	−5.86
12	−3.046	−3.046	7.37	−5.13
Model[14]	—	—	7.22	−5.16

values of EA_1 and ΔE_1 for all high activity compounds (compounds **1**–**7**, **9**, and **10**) are in the same range, that is, 4.59–4.78 kcal/mol and −9.12 to −9.80 kcal/mol, respectively. For the low activity compounds (compounds **8**, **11**, and **12**), the EA_1 and ΔE_1 are between 7.29 to 7.37 and −5.13 to −6.70 kcal/mol. Remarkably, most compounds with low EA_1 and ΔE_1 (high activity) have substituent groups at the β-C_9 position (R_2), while all compounds with high EA_1 and ΔE_1 (low activity) have large substituents at the C_3 position (R_1). Therefore, the position of substituent appears to have significant effect on EA_1 and ΔE_1 and hence on the activities. The EA_1 and ΔE_1 energies of the model system are 7.22 and −5.16 kcal/mol,[14] which are very close to those of low activity compounds. This indicates that the model system exhibits the same characteristic as low activity compounds and hence tends to be an inactive compound if exists.

2.2. Homolytic C–C cleavage (pathway 2)

For all 12 compounds, some important structural parameters of radical 2A, racial 2B, and transition state TS_2 are given in Table 4 and their optimized structures shown in Figure 4. All the structural parameters of each compound are similar. No significant difference is observed. The C_3–C_4 distance is obviously increasing as the reaction proceeds, that is, from around 1.6 Å in 2A to around 2.0 Å in TS_2 and to 3.3–3.4 Å in 2B. The decrease in C_4–C_5–C_{5a}–C_{12a} dihedral angle of around 21.9–23.0° and the increase in C_3–O_{13}–C_{12}–C_{12a} dihedral angle of around 31.0–32.7° from radicals 2A to 2B indicate that the increasing of C_3–C_4 distance is also facilitated by the rotation of these two angles.

The activation energy of pathway 2 (EA_2) and the energy difference between radical 2A and 2B (ΔE_2) for all 12 artemisinin compounds and the model system are shown in Table 5. Unlike the pathway 1, no significant difference in energy values among high and low activity compounds was detected. The energy values of EA_2 and ΔE_2 for all compounds are in the range of 4.36–5.99 kcal/mol and −7.41 to −10.20 kcal/mol, respectively. Therefore, the substituent groups at either C_3 or C_9 positions do not change the pattern of both EA_2 and ΔE_2 energies.

2.3. Comparison between the two pathways

The energy differences between radical 1A and 2A, $\Delta E(1A - 2A)$, and between radical 1B and 2B,

Table 4. Important structural parameters of radical 2A, transition state (TS_2), and radical 2B in pathway 2; distances in Angstroms and angles in degrees

		1	2	3	4	5	6	7	8	9	10	11	12	Model
C_3–C_4	2A	1.600	1.604	1.599	1.599	1.599	1.599	1.600	1.599	1.599	1.605	1.598	1.596	1.640
	TS_2	1.968	1.968	1.967	1.965	1.966	1.966	1.967	1.968	1.967	1.949	1.971	1.986	1.947
	2B	3.324	3.293	3.302	3.297	3.302	3.305	3.295	3.314	3.296	3.369	3.308	3.305	3.843
O_2–C_3	2A	1.335	1.334	1.336	1.336	1.336	1.336	1.335	1.335	1.335	1.335	1.335	1.335	1.326
	TS_2	1.256	1.256	1.257	1.257	1.257	1.257	1.257	1.256	1.256	1.259	1.255	1.254	1.262
	2B	1.213	1.213	1.213	1.213	1.213	1.213	1.213	1.214	1.214	1.215	1.213	1.212	1.212
O_2–C_3–O_{13}	2A	116.4	116.5	116.4	116.4	116.4	116.4	116.4	116.1	116.1	116.5	116.0	116.0	118.3
	TS_2	122.7	122.7	122.7	122.7	122.7	122.7	122.7	122.5	122.5	122.5	122.5	122.8	123.0
	2B	125.8	125.8	125.8	125.8	125.8	125.8	125.8	125.4	125.4	125.3	125.4	125.7	126.4
O_2–C_3–O_{13}–C_{12}	2A	48.8	48.9	49.3	49.1	49.4	49.1	49.0	48.3	48.5	44.5	49.3	49.7	40.3
	TS_2	27.8	27.9	28.1	28.0	28.0	28.0	28.0	27.9	27.8	25.1	28.0	27.9	26.4
	2B	−14.2	−13.4	−14.0	−13.8	−14.1	−14.1	−13.6	−14.8	−14.3	−18.4	−14.3	−14.4	−2.18
C_4–C_5–C_{5a}–C_{12a}	2A	328.1	327.9	328.0	327.9	327.7	327.7	327.9	327.6	327.5	327.1	327.5	327.3	325.9
	TS_2	323.7	323.4	323.6	323.6	323.6	323.6	323.7	323.4	323.3	323.9	323.4	323.1	321.2
	2B	305.1	305.6	305.5	305.5	305.8	305.7	305.6	305.4	305.4	304.5	305.2	305.4	295.4
C_3–O_{13}–C_{12}–C_{12a}	2A	43.6	43.6	43.3	43.2	43.0	43.0	43.2	43.3	43.3	44.0	42.9	42.6	51.3
	TS_2	53.8	53.7	53.5	53.4	53.6	53.6	53.5	53.5	53.4	54.1	53.5	53.7	58.6
	2B	75.2	75.1	75.1	75.2	75.4	75.4	75.1	75.4	75.3	75.0	75.1	75.3	85.4

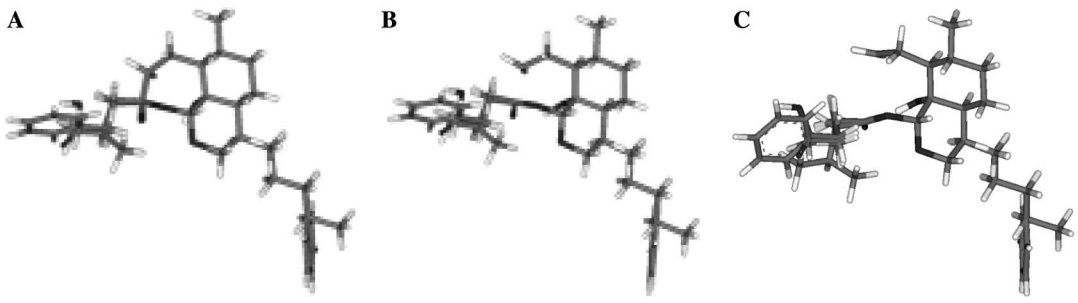

Figure 4. Optimized structures of the (A) O-centered radical 2A, (B) transition state TS_2, and (C) C-centered radical 2B in pathway 2 for all 12 compounds.

Table 5. Activation energy (EA_2) and energy difference between radical 2A and 2B (ΔE_2) in pathway 2

No	log (D-6)	log (W-2)	EA_2 (kcal/mol)	ΔE_2 (kcal/mol)
1	0.819	0.754	5.07	−8.52
2	0.375	0.279	5.99	−7.54
3	0.961	0.668	5.11	−8.55
4	0.675	0.740	5.10	−8.54
5	1.765	1.320	5.08	−8.53
6	0.230	0.161	5.08	−8.53
7	1.705	1.399	5.06	−8.56
8	−1.000	−1.000	5.19	−8.32
9	0.859	0.836	5.13	−8.51
10	0.262	0.398	4.36	−10.20
11	−1.222	−1.699	5.23	−8.06
12	−3.046	−3.046	5.63	−7.41
Model[14]	—	—	7.76	−10.07

Table 6. Energy difference between radical 1A and 2A, ΔE(1A − 2A), and between radical 1B and 2B, ΔE(1B − 2B)

Compound	log (D–6)	log (W-2)	ΔE(1A − 2A) (kcal/mol)	ΔE(1B − 2B) (kcal/mol)
1	0.819	0.754	+3.68	+2.45
2	0.375	0.279	+4.57	+2.42
3	0.961	0.668	+3.70	+2.54
4	0.675	0.740	+3.71	+2.52
5	1.765	1.320	+3.68	+2.49
6	0.230	0.161	+3.67	+2.50
7	1.705	1.399	+3.72	+2.48
8	−1.000	−1.000	+0.80	+2.42
9	0.859	0.836	+3.33	+2.72
10	0.262	0.398	+4.02	+4.84
11	−1.222	−1.699	+0.26	+2.46
12	−3.046	−3.046	−0.328	+1.95
Model[14]	—	—	+1.51	+6.42

ΔE(1B − 2B), for all compounds were computed (Table 6) to access the competitiveness of each pathway. In addition, the energy schemes for both pathways of high and low activity compounds are shown in Figure 5.

It is clearly seen that the high activity compounds have higher ΔE(1A − 2A), 3.33–4.57 kcal/mol (Fig. 5A), while the low activity compounds have lower values, −0.328 to 0.80 kcal/mol (Fig. 5B). This indicates that the more stable 2A radical is very likely to be a requirement for high antimalarial activity and it also emphasizes the importance of the pathway 2 over the pathway 1. Considering the C-centered radicals, the energy of radical 2B in all compounds is also lower than that of radical 1B, ΔE(1B − 2B) of 1.95 to 4.84 kcal/mol.

2.4. Relationship to biological activity

As the main objective of this study was to investigate relationship(s) between biological activity and calculated properties, all energy data (EA_1, ΔE_1, EA_2, ΔE_2, ΔE(1A − 2A), and ΔE(1B − 2B)) and some important structural parameters presented in Tables 2 and 4 were considered. The relationships were investigated by plotting all the properties against activities. For the structural parameters, no relationship with activities was found. However, three energy parameters, that is, EA_1, ΔE_1, and ΔE(1A − 2A), have significant relations with antimalarial activities. Their relationships are shown in Figures 6–8.

Considering the activation energy for pathway 1 (EA_1), compounds with low EA_1 have high activities (see Fig. 6). Since the EA_1 refers to the ease in proceeding along reaction of pathway 1, radical 1B seems to be an important species for high activities.

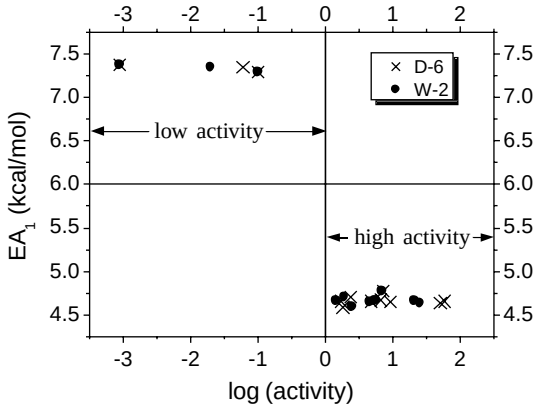

Figure 6. Relationship between log (activities) and EA_1 for 12 artemisinin derivatives.

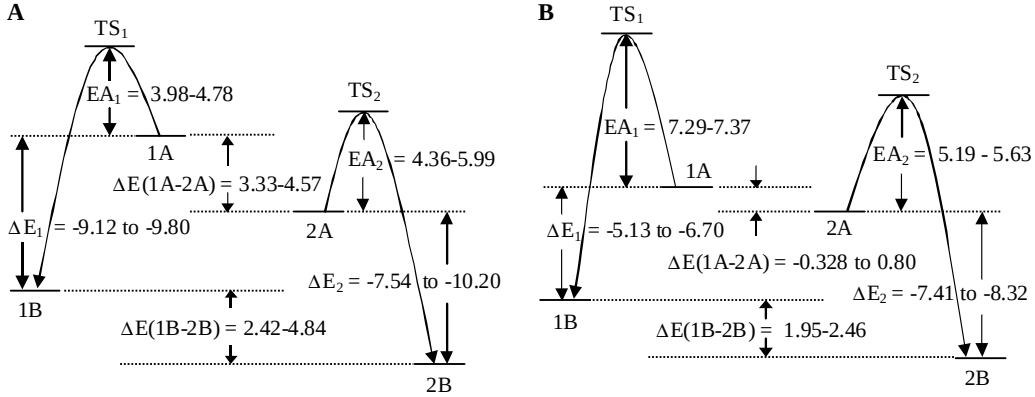

Figure 5. Schematic energy scheme for the mechanism of action for (A) nine high activity artemisinin derivatives and (B) three low activity artemisinin derivatives (except for compound **12** that has 1A energy slightly lower than 2A energy). All values are in kcal/mol unit.

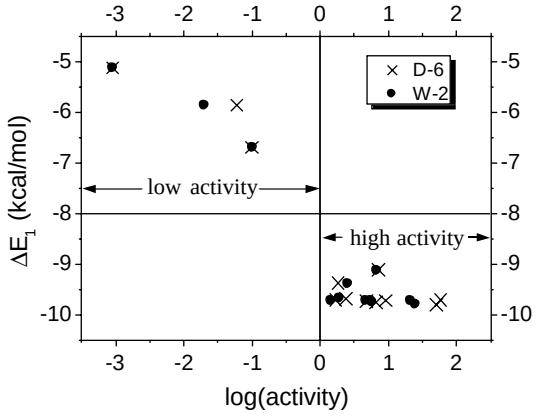

Figure 7. Relationship between log (activities) and ΔE_1 for 12 artemisinin derivatives.

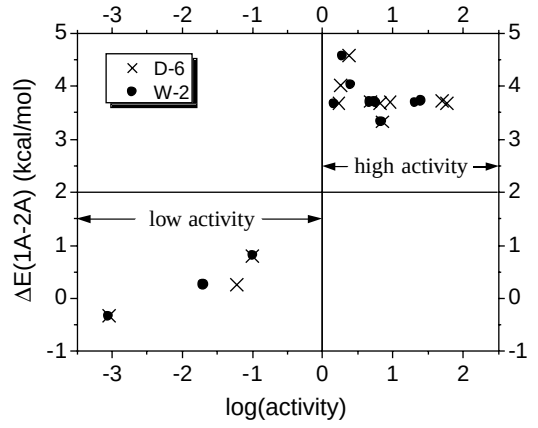

Figure 8. Relationship between log (activities) and $\Delta E(1A - 2A)$ for 12 artemisinin derivatives.

For the ΔE_1 parameter, compounds with a lower ΔE_1 have higher activities (see Fig. 7). This once again points out that radical 1B is essential for high activities because the ΔE_1 refers to the ease of radical 1B formation.

In the case of $\Delta E(1A - 2A)$ parameter (Fig. 8), high activity compounds have high $\Delta E(1A - 2A)$ values, that is, radical 2A is more stable than radical 1A. This implies that the energetically more preferable pathway 2 is also of importance for high activities.

3. Conclusions

The theoretical investigations on the reactions, leading to the formation of C_4 free radicals in pathways 1 and 2 for the mode of action of 12 artemisinin compounds using the IMOMO(B3LYP/6-31G(d,p):HF/3-21G) method, reveal that both the homolytic C–C cleavage reaction (pathway 2) and the intramolecular 1,5-hydrogen shift process (pathway 1) are important for antimalarial activities. For high activity compounds, radical 2A is energetically more stable than radical 1A; therefore, the compound will mainly proceed along the pathway 2, indicating the crucial role of this pathway. This is also well in agreement with the docking results between artemisinin compounds and heme that illustrate the preference of heme iron to approach the O_1 atom at the endoperoxide linkage of artemisinin compounds.[2,16] On the other hand, compounds with low EA_1 energy and high ΔE_1 energy, a case that indicates the ease of intramolecular 1,5-hydrogen shift reaction in the pathway 1, have high antimalarial activities, thus radical 1B tends to be an important species reinforcing the activities.

Moreover, the EA_1, ΔE_1, and $\Delta E(1A - 2A)$ have good relationships with antimalarial activities, which could be used to effectively distinguish high activity compounds from low activity compounds. This information is very helpful for the drug discovery and development process. In addition, the results have reconfirmed that the use of 6,7,8-trioxybicyclo[3,2,2]nonane as a representative compound of artemisinin systems for the studies of mechanism of action is certainly inappropriate.[11] The main reason is that it exhibits the same energetic profiles as those of the low activity artemisinin compounds.

4. Experimental

4.1. Biological data

The structures and biological activities of 12 artemisinin compounds were taken from the literature.[12] The antimalarial activities were measured as the IC_{50} values, the inhibitory concentration of a compound required for 50% inhibition of the parasitemia, against the Sierra Leone (D-6) and the Indochina (W-2) clones of *Plasmodium falciparum*. The D-6 clone is mefloquine-resistant but chloroquine-sensitive, while the W-2 clone is chloroquine-resistant but mefloquine-sensitive. Moreover, the antimalarial activities were reported as the relative scale to those of artemisinin to reduce any inconsistency among different environments in the experiments. Compounds, which are more potent than artemisinin, that is, log (activity) > 0.0, are denoted as 'high activity compounds', whereas compounds, which are less active than artemisinin, that is, log (activity) < 0.0, are denoted as 'low activity compounds'.

4.2. Computational methods

Our previous results[11] have shown that the IMOMO method[17] employing HF/3-21G and B3LYP/6-31G(d,p) levels gave better quality of structural parameters than the pure HF/3-21G method and even better than the B3LYP/6-31G(d,p) level itself, as compared to the X-ray data. Therefore, this method was chosen for structural optimizations of all compounds used in this study. The 6,7,8-trioxybicylco[3,2,2]nonane substructure together with the O_{11} atom was used as the model system and the artemisinin compounds were used as the real system. The model system, which contains atoms involved in the free radical formation, was treated at the highly accurate level of theory, B3LYP/6-31G(d,p), whereas the real system was treated at HF/3-21G. Using this approach, geometries of 12

artemisinin derivatives, and their corresponding free radicals (1A, 1B, 2A, and 2B) and transition states (TS_1 and TS_2) were fully optimized. Furthermore, frequency calculations at the same level were additionally carried out to confirm the optimized transition state structures. All quantum chemical calculations were performed using the Gaussian 98 program.[18]

Acknowledgments

The authors thank the Austrian-Thai Center for Computer Assisted Chemical Education and Research (ATC) and the Computational Chemistry Unit Cell (CCUC), Department of Chemistry, Faculty of Science, Chulalongkorn University, Thailand, for providing computing resources and other research facilities.

References and notes

1. Roll Back Malaria, World Health Organization, and UNICEF, World Malaria Report 2005.
2. Tonmunphean, S.; Parasuk, V.; Kokpol, S. *Quant. Struct.-Act. Rel.* **2000**, *19*, 475.
3. Tonmunphean, S.; Kokpol, S.; Parasuk, V. *J. Sci. Res. Chula. Univ.* **2004**, *29*, 1.
4. Krungkrai, S. R.; Yuthavong, Y. *Trans. R. Soc. Trop. Med. Hyg.* **1987**, *81*, 710.
5. Brossi, A.; Venugopalan, B.; Gerpe, L. D.; Yeh, H. J.; Flippen-Anderson, J. L.; Buchs, P.; Luo, X. D.; Milhous, W.; Peters, W. *J. Med. Chem.* **1988**, *31*, 645.
6. Meshnick, S. R. *Int. J. Parasitol.* **2002**, *32*, 1655, and references therein.
7. Meshnick, S. R.; Yang, Y.-Z.; Lima, V.; Kuypers, F.; Kamchonwongpaisan, S.; Yuthavong, Y. *Antimicrob. Agents Chemother.* **1993**, *37*, 1108.
8. Kamchonwongpaisan, S.; Meshnick, S. R. *Gen. Pharmacol.* **1996**, *27*, 587.
9. Asawamahasakda, W.; Ittarat, I.; Pu, Y.-M.; Ziffer, H.; Meshnick, S. R. *Antimicrob. Agents Chemother.* **1994**, *38*, 1854.
10. Posner, G. H.; Oh, C. H. *J. Am. Chem. Soc.* **1992**, *114*, 8328.
11. Tonmunphean, S.; Parasuk, V.; Kokpol, S. *J. Mol. Struct. (THEOCHEM)* **2005**, *724*, 99.
12. Avery, M. A.; Mehrotra, S.; Johnson, T. L.; Bonk, J. D.; Vroman, J. A.; Miller, R. *J. Med. Chem.* **1996**, *39*, 4149.
13. Gu, J.; Chen, K.; Jiang, H.; Leszczynski, J. *J. Mol. Struct. (THEOCHEM)* **1999**, *491*, 57.
14. Gu, J.; Chen, K.; Jiang, H.; Leszczynski, J. *J. Phys. Chem. A* **1999**, *103*, 9364.
15. Wu, W.-M.; Wu, Y.; Wu, W.-L.; Yao, Z.-J.; Zhou, C-M.; Li, Y.; Shan, F. *J. Am. Chem. Soc.* **1998**, *120*, 3316.
16. Tonmunphean, S.; Parasuk, V.; Kokpol, S. *J. Mol. Model.* **2001**, *7*, 26.
17. Humbel, S.; Sieber, S.; Morokuma, K. *J. Chem. Phys.* **1996**, *105*, 1959.
18. Frisch, M. J.; Trucks, G. W.; Schlegel, H. B.; Scuseria, G. E.; Robb, M. A.; Cheeseman, J. R.; Zakrzewski, V. G.; Montgomery, Jr., J. A.; Stratmann, R. E.; Burant, J. C.; Dapprich, S.; Millam, J. M.; Daniels, A. D.; Kudin, K. N.; Strain, M. C.; Farkas, O.; Tomasi, J.; Barone, V.; Cossi, M.; Cammi, R.; Mennucci, B.; Pomelli, C.; Adamo, C.; Clifford, S.; Ochterski, J.; Petersson, G. A.; Ayala, P. Y.; Cui, Q.; Morokuma, K.; Salvador, P.; Dannenberg, J. J.; Malick, D. K.; Rabuck, A. D.; Raghavachari, K.; Foresman, J. B.; Cioslowski, J.; Ortiz, J. V.; Baboul, A. G.; Stefanov, B. B.; Liu, G.; Liashenko, A.; Piskorz, P.; Komaromi, I.; Gomperts, R.; Martin, R. L.; Fox, D. J.; Keith, T.; Al-Laham, M. A.; Peng, C. Y.; Nanayakkara, A.; Challacombe, M.; Gill, P. M. W.; Johnson, B.; Chen, W.; Wong, M. W.; Andres, J. L.; Gonzalez, C.; Head-Gordon, M.; Replogle, E. S.; Pople, J. A. Gaussian 98, Revision A.11, Gaussian: Pittsburgh PA, 2001.